

each time it passes through a different medium, which would occur when flying through rain, for example. Sensing during rain and at low angles of incidence need further investigation.

Acknowledgment

This work was supported by the NASA Center for Aerospace Research at North Carolina A&T State University under Grant NCC-1-255. Instrumentation was partly from an AFOSR Instrumentation Grant. David E. Oliver of Polytec PI provided information on the operation of the laser vibrometer. This support is gratefully acknowledged.

References

- ¹Abraham, R. H., and Shaw, C. D., "Dynamics—The Geometry of Change," *Periodic, Chaotic, Global, and Bifurcation Behavior*, Vol. 1, Aerial Press, Santa Cruz, CA, 1988, pp. 115–197.
- ²Thompson, J. M. T., *Instabilities and Catastrophes in Science and Engineering*, Wiley, New York, 1982.
- ³Hirsch, M. W., and Smale, S., *Differential Equations, Dynamical Systems and Linear Algebra*, Academic Press, New York, 1974.
- ⁴Guckenheimer, J., and Holmes, P., *Nonlinear Oscillations, Dynamical Systems and Bifurcations of Vector Fields*, Springer-Verlag, New York, 1983.
- ⁵Dowell, E. H., and Llgamor, M., *Studies in Nonlinear Aerolasticity*, Springer-Verlag, New York, 1988.
- ⁶Edwards, J. W., and Malone, J. B., "Current Status of Computational Methods for Transonic Unsteady Aerodynamics and Aeroelastic," *Computing Systems in Engineering*, Vol. 3, No. 5, 1992, pp. 545–569.
- ⁷Theodorsen, T., "General Theory of Aerodynamic Instability and the Mechanism of Flutter," NACA Rept. 496, 1935.
- ⁸Sears, W. R., "Some Aspects of Non-Stationary Airfoil Theory and Its Practical Application," *Journal of Aeronautical Science*, Vol. 8, 1941, pp. 104–108.
- ⁹Chen, P., Liu, C., Sarhaddi, D., Karpel, D., Idan, M., and Jung, S., "Development of Aerodynamic and Aeroelastoclastic Modules in ASTROS," AF/STTR Phase II Final Rept., Vols. 1–8, ZONA Technology, 1999.
- ¹⁰Derham, R., and Hagood, N., "Rotor Design Using Smart Materials to Actively Twist Blades," *Proceedings of the American Helicopter Society 52nd Annual Forum*, Vol. 2, American Helicopter Society, Washington, DC, 1996, pp. 1242–1252.
- ¹¹Wilkie, W. K., "Anisotropic Piezoelectric Twist Actuation of Helicopter Rotor Blades: Aeroelastic Analysis and Design Optimization," Ph.D. Dissertation, College of Engineering, Univ. of Colorado, Boulder, CO, 1997.
- ¹²Rosenbaum, R., and Scalan, R., "A Note on Flight Flutter Testing," *Journal of Aeronautical Science*, Vol. 15, 1948, pp. 366–370.
- ¹³Fung, Y. C., *Biomechanics: Circulation*, Springer-Verlag, New York, 1997.
- ¹⁴Heeg, J., "Analytical and Experimental Investigation of Flutter Suppression by Piezoelectric Actuation," NASA TP 3241, NASA Langley Research Center, Feb. 1993.
- ¹⁵Crawley, E. F., and deLuis, J., "Use of Piezoelectric Actuators as Elements of Intelligent Structures," *AIAA Journal*, Vol. 25, No. 10, 1987, pp. 1373–1385.
- ¹⁶Langley International Forum on Aeroelasticity and Structural Dynamics, *Proceedings: Part I*, Paper 19990050911, NASA Langley Research Center, Hampton, VA, 1999.
- ¹⁷Langley International Forum on Aeroelasticity and Structural Dynamics, *Proceedings: Part II*, Paper 19990052675, NASA Langley Research Center, Hampton, VA, 1999.
- ¹⁸MATLAB, Math Works, Natick, MA.
- ¹⁹"QUICKPACK Piezoelectric Actuators," Active Control eXperts, Cambridge, MA, 1997.
- ²⁰Laser Vibrometer Users Manual, Polytec PI, Auburn, MA.
- ²¹Ghoshal, A., Wheeler, E. A., AshokKumar, C. R., Sundaresan, M. J., Schulz, M. J., Human, M., Pai, P. F., "Vibration Suppression Using a Laser Vibrometer and Piezoceramic Patches," *Journal of Sound and Vibration*, Vol. 235, No. 2, 2000, pp. 261–280.
- ²²Asok Kumar, C. R., Ghoshal, A., Sundaresan, M. J., Schulz, M. J., and Human, M., "Vibration Suppression Using Reconfigurable Coordinate Velocities," *International Journal of Mechanics and Control*, Vol. 3, No. 2, 2003.
- ²³Inman, D. J., "Nonlinear Vibrations," *Engineering Vibration*, Prentice-Hall, Englewood Cliffs, NJ, 1996, Chap. 10.
- ²⁴"Laser Radar Remote Sensing Vibrometer," Coherent Technologies, Lafayette, CO. URL: <http://sbir.nasa.gov/SBIR/successes/ss/4-006text.html> [cited 20 April 2005].

E. Livne
Associate Editor

Preliminary Analysis of Nonlinearity in Military Jet Aircraft Noise Propagation

Kent L. Gee,* Thomas B. Gabrielson,[†]
Anthony A. Atchley,[‡] and Victor W. Sparrow[§]
Pennsylvania State University,
University Park, Pennsylvania 16802

Introduction

THE role of nonlinearity in the propagation of noise radiated from high-performance jet aircraft is currently not well understood, despite past studies such as those by Blackstock¹ and Howell and Morfey (see Refs. 2 and 3). More recently, Norum et al.⁴ found that F-15 flyover data exhibited anomalously high spectral levels above 1.5 kHz; although nonlinear effects were mentioned as a possible cause for the high levels, the issue was not pursued further. As a finite amplitude noise waveform propagates, it undergoes amplitude-dependent steepening, which results in a transfer of spectral energy from mid- to higher frequencies. If competing processes, such as atmospheric absorption and geometrical spreading, are not sufficient to prevent shock formation, coalescence of shocks will also transfer energy to lower frequencies.⁵ Significant nonlinear spectral broadening, if present in high-speed jet noise, would cause perceived levels to vary from those predicted via linear methods.

The purpose of this Note is to describe a preliminary analysis of F/A-18E Super Hornet static engine run-up noise measurements that shows evidence of nonlinear propagation effects. Following a summary of the measurement, results of power spectral density (PSD) and waveform statistical calculations are presented. Evidence of nonlinear propagation is demonstrated by a comparison of measured spectra with free-field linear predictions and by calculation of a nonlinear indicator derived by Howell and Morfey (see Refs. 2 and 3).

Measurement Summary

The F/A-18E run-up measurements were conducted at the U.S. Naval Air Engineering Station, Lakehurst, New Jersey, during the evening of 15 April 2003. Recordings were made with both engines idling (Idle), at military thrust (Mil), and with afterburners engaged (AB). During the tests, the approximate ambient temperature and relative humidity were 20°C and 50%, and average wind speeds were relatively low, approximately 3 m/s at a height of 4.5 m. The monitored wind direction, as well as a temperature inversion measured near the ground just before the tests, suggests that the atmosphere was slightly downward refracting. Data were acquired at 18, 74, and 150 m from the engine nozzles along a radial line 135 deg from the forward direction, which is approximately the peak directivity angle for the F/A-18E at high-thrust conditions. The 18-m data were acquired with a 6.35-mm Bruel and Kjaer 4938 condenser microphone flush mounted in an aluminum plate baffle located horizontally on

Received 28 April 2004; presented as Paper 2004-3009 at the AIAA/CEAS 10th Aeroacoustics Conference, Manchester, England, United Kingdom, 10–12 May 2004; revision received 5 January 2005; accepted for publication 6 January 2005. Copyright © 2005 by the American Institute of Aeronautics and Astronautics, Inc. All rights reserved. Copies of this paper may be made for personal or internal use, on condition that the copier pay the \$10.00 per-copy fee to the Copyright Clearance Center, Inc., 222 Rosewood Drive, Danvers, MA 01923; include the code 0001-1452/05 \$10.00 in correspondence with the CCC.

*Ph.D. Candidate, Graduate, Program in Acoustics, 202 Applied Science Building; kengtee@psu.edu. Student Member AIAA.

[†]Senior Research Associate, Applied Research Laboratory, Post Office Box 30, State College, PA 16804.

[‡]Professor of Acoustics and Chair, Graduate Program in Acoustics, 217 Applied Science Building. Member AIAA.

[§]Associate Professor of Acoustics, Graduate Program in Acoustics, 316B Leonhard Building. Senior Member AIAA.

pavement. The 74- and 150-m data were acquired with handheld Endeveco 8510C-15 piezoresistive pressure transducers located about 1.2 m above grassy ground. All data were recorded with portable Sony TCD-D8 digital audio tape recorders sampling at 44.1 kHz. Approximately 12 s of the recorded waveforms for each condition have been used in obtaining the results presented hereafter.

Results

Power Spectral Measurements

In Figs. 1–3 the PSD at the three measurement locations is shown for each of the engine conditions. In Fig. 1, the overall sound pressure levels (OASPL) for AB, Mil, and Idle at 18 m are 151, 147, and 99 dB, respectively. Note that these and other OASPL calculations given hereafter are referenced to $20 \mu\text{Pa}$. Because the Idle spectrum reaches the system noise floor at approximately 6 kHz, additional analysis of those data is restricted to below that limit. For the latter two distances, 74 and 150 m, shown in Figs. 2 and 3, the Idle levels are largely below their respective noise floors and are not meaningful measurements. The irregular nature of the noise floors above 1 kHz in Figs. 2 and 3, which are shown as a noise equivalent PSD, is caused by an experimentally determined diffraction correction applied to the Endeveco sensor data. Because of uncertainty in the accuracy of the diffraction correction at high frequencies, the PSD calculations and all other analyses have been limited to below 10 kHz. The OASPL at 74 m are 135 and 132 dB for the AB and Mil engine settings. By 150 m, the OASPL for AB and Mil conditions are reduced to 127 and 123 dB, respectively.

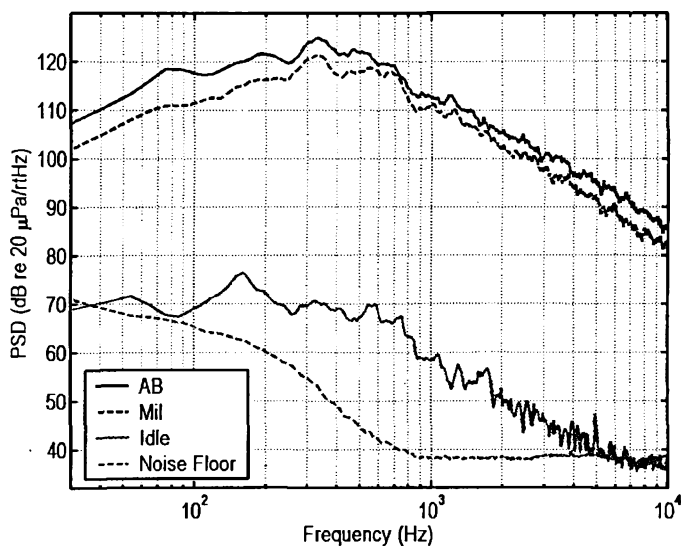


Fig. 1 PSD in decibels referred to $20 \mu\text{Pa}/\sqrt{\text{Hz}}$, at 18 m. The OASPL of spectra at AB, Mil, and Idle are 151, 147, and 99 dB, respectively.

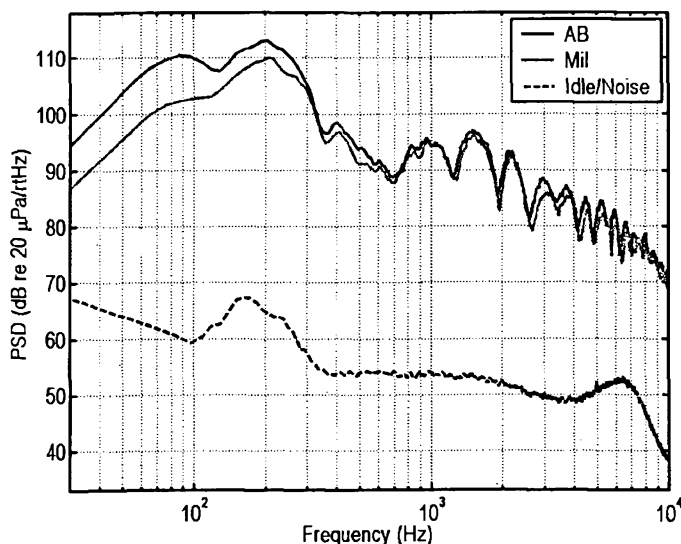


Fig. 2 PSD at 74 m for measured engine conditions. The OASPL of spectra at AB and Mil are 135 and 132 dB, respectively.

Table 1 Skewness S and kurtosis K for engine conditions and measurement locations^a

Condition and location	S	K
Idle, 18 m	-0.01	3.05
Mil, 18 m	0.38	3.13
Mil, 74 m	0.25	3.25
Mil, 150 m	0.08	2.99
AB, 18 m	0.60	3.40
AB, 74 m	0.39	3.41
AB, 150 m	0.26	3.05

^aFor ideally Gaussian data, $S = 0$ and $K = 3$.

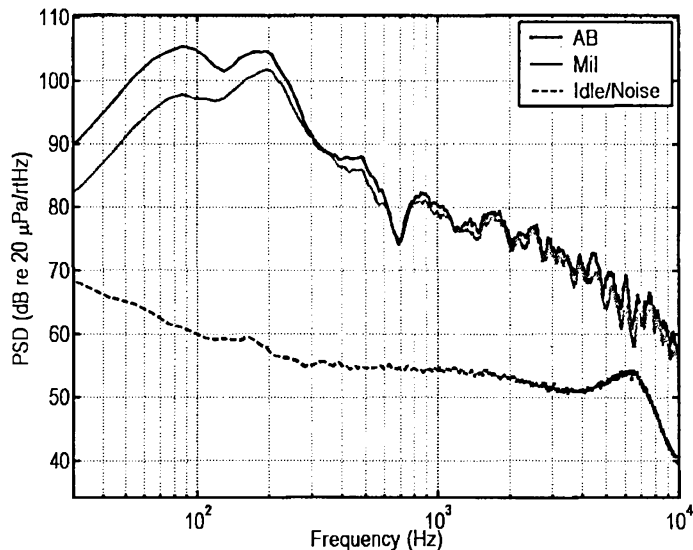


Fig. 3 PSD at 150 m for measured engine conditions. The OASPL for AB and Mil are 127 and 123 dB, respectively.

The 74- and 150-m spectral measurements exhibit multiple dips in level of several decibels, and, although not readily apparent from the logarithmic frequency scale, the dips occur at roughly regular intervals of approximately 600–700 Hz. These dips are likely indicative of multipath interference, for example, ground reflections; however, considerable terrain inhomogeneity over the measurement range has precluded meaningful quantitative analysis of the phenomenon. However, if the multipath hypothesis holds, it is noteworthy that the offset between AB and Mil dip frequencies, which increases as a function of frequency, is possible evidence that the dominant acoustic source region in the jets changes between the two engine conditions.

Statistical Calculations

The skewness S and kurtosis K , which are the normalized third and fourth central moments of the probability density function, have been calculated for each of the measurement locations and engine conditions. The value of S , which is a measure of the asymmetry of the data distribution, has been used to quantify the phenomenon known as crackle.^{6,7} No physical phenomenon has been correlated with K , which describes the peaked nature of the distribution. Calculation of these moments has been performed because the non-Gaussian nature of the time series data is a necessary (but not sufficient) condition of nonlinear system identification.⁸ In other words, if the calculated normalized moments for a given measured waveform deviate from expected Gaussian values, for example, $S = 0$ and $K = 3$, the propagation is possibly nonlinear.

To limit waveform frequency content to below 10 kHz for these statistical calculations, a digital eighth-order Butterworth low-pass filter with a cutoff frequency of 10 kHz (6 kHz for the 18-m Idle data) was first applied to the time series. The statistical results for the various measurement locations and engine settings are listed in Table 1. The AB and Mil propagation is non-Gaussian over the measurement range, although it becomes less so by 150 m, especially for the Mil power case. Finally, although its significance is currently unknown, note that K increases between 18 and 74 m for

Mil power and remains essentially constant for the AB case, whereas S decreases for both engine settings over the same range.

Evidence of Nonlinear Propagation Effects

Observation of the non-Gaussian nature in the AB and Mil time series data demonstrates that the propagation may, in fact, be nonlinear over the measurement range. Two additional analyses of the data reveal evidence that the propagation is indeed nonlinear.

Comparison of Linear Extrapolations with Measurement

Free-field linear extrapolation of the 18- and 74-m measured spectra out to 150 m have been calculated by applying the expected small-signal power loss due to 1) spherical spreading and 2) atmospheric absorption.⁹ Mid- to high-frequency comparisons between the linearly extrapolated and the measured spectra for the Mil and AB cases are shown in Figs. 4 and 5, respectively. The linear frequency scale has been chosen to emphasize clearly the differences between linearly predicted and measured levels. The comparisons for frequencies below 1 kHz are not displayed because the reasons for a downward shift in Mil and AB spectral peak frequencies between 18 and 74 m (Figs. 1 and 2) are not clearly understood. Whereas shock coalescence may, in fact, contribute to this shift, it is unclear whether the assumptions of aeroacoustic compactness and, thus, spherical spreading, are valid at 18 m for low frequencies. If they are invalid, the 18-m extrapolation is somewhat erroneous at frequencies for which nonspherical spreading occurs. Furthermore, the location in frequency of the first spectral dip at 74 m may significantly exaggerate the apparent peak frequency shift. For these reasons, only comparisons above 1 kHz are shown.

Examination of Figs. 4 and 5 shows excess power at high frequencies for the measured Mil and AB spectra as compared to the extrapolated spectra. For example, in Fig. 4 at 10 kHz, the difference is 12 dB from the 18-m extrapolation and 4 dB from the 74-m extrapolation. Furthermore, the trends in spectral levels indicate less power measured at 150 m than linearly predicted for frequencies below a few kilohertz. When combined, these spectral changes are characteristic of the nonlinear propagation of noise.⁵ Also note that the spectral energy transfer appears to be less significant between 74 and 150 m, which is not surprising because as waveform amplitudes are reduced by atmospheric absorption and geometrical spreading, additional nonlinear distortion of the propagating waveform will also lessen.

Howell–Morfey Nonlinearity Indicator

In their effort to predict the evolution of a finite amplitude jet noise spectrum, Howell and Morfey derived an equation for the PSD as a function of range that predicts the occurrence of nonlinear propagation effects only if Q_{p^2p} , a third-order spectral quantity, is nonzero. [See Eq. (5) of Ref. 2.] Thus, nonlinear energy transfer

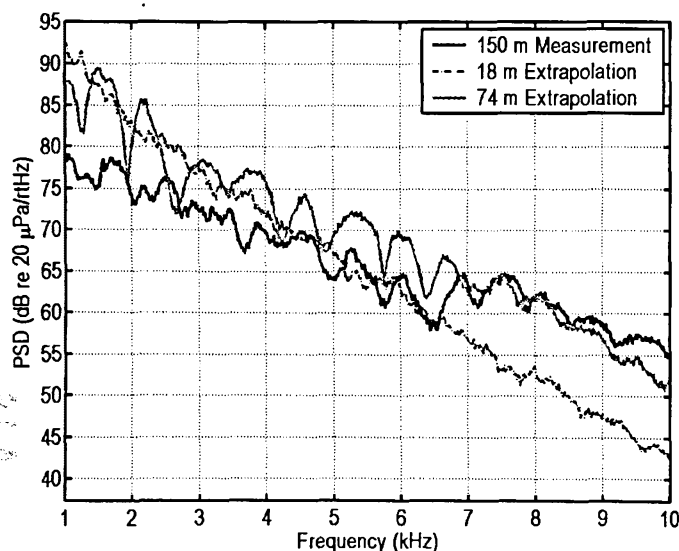


Fig. 4 Comparison of linearly extrapolated spectra from 18 and 74 m with the 150-m Mil power measurement between 1 and 10 kHz.

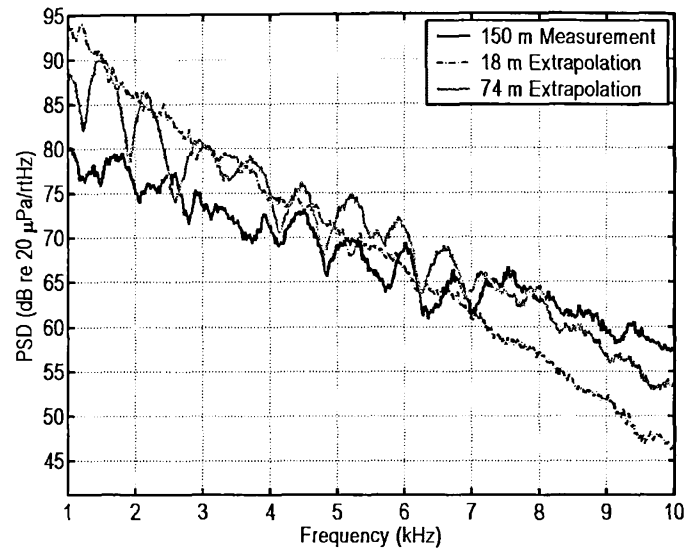


Fig. 5 Comparison of linearly extrapolated spectra from 18 and 74 m with the 150-m AB measurement between 1 and 10 kHz.

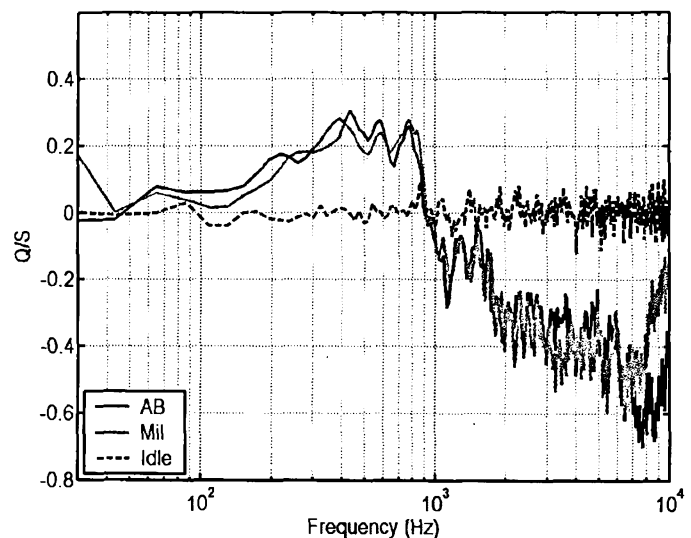


Fig. 6 Howell–Morfey nonlinearity indicator Q/S calculated for three engine conditions at 18 m; Idle calculation is only physically significant below 6 kHz, where measured levels are above system noise floor.

at a given location may be readily identified by a nonzero Q_{p^2p} measurement. Q_{p^2p} is defined as the imaginary part of the cross-spectral density between the pressure squared and the pressure and may be written as

$$Q_{p^2p}(\omega) = \text{Im}\{\mathfrak{F}\{p^2(t)\}\mathfrak{F}^*\{p(t)\}\}$$

where \mathfrak{F} , the asterisk, and (\cdot) , respectively, represent Fourier transform, complex conjugation, and ensemble-average operators. Howell and Morfey's nonlinearity indicator, a nondimensional ratio dubbed Q/S , is derived by normalizing Q_{p^2p} by the PSD, multiplied by the root-mean-square pressure. McInerney and Olcmen¹⁰ have recently calculated Q/S in the context of identification of nonlinear propagation effects in rocket noise.

The indicator Q/S has the following physical interpretation. If $Q/S < 0$ for a given frequency, the amount of power at that frequency is increasing due to energy transfer from other frequencies. If $Q/S > 0$, the opposite is true; energy is being transferred to other frequencies and the amount of power is decreasing. Finally, if $Q/S = 0$, it is because $Q_{p^2p} = 0$; therefore, no nonlinear interaction exists. In Fig. 6, Q/S is plotted from the 18-m measurements of AB, Mil, and Idle conditions. Not surprisingly, the Q/S for Idle approaches zero, which means that no nonlinear energy transfer is occurring. This could also have been predicted simply from the fact that all odd-order spectra are zero for a statistically Gaussian signal and that the 18-m Idle data are essentially Gaussian (Table 1).

Q/S is significantly different for the Mil and AB data in Fig. 6. There are two main frequency regions in which the ratio has opposite

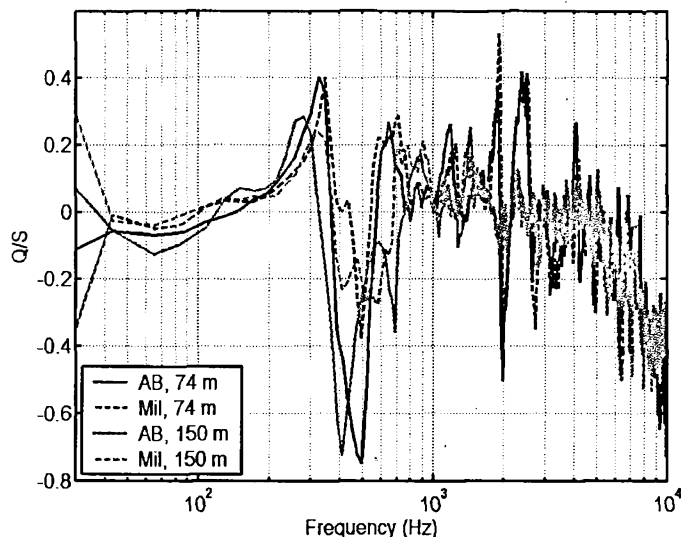


Fig. 7 Howell-Morfe nonlinearity indicator Q/S at 74 and 150 m; large peaks and sharp sign changes appear to be related to spectral dips evident in PSD measurements.

signs, indicating that nonlinear propagation effects are present. From approximately 60 Hz to 1 kHz, energy is being transferred upward in the spectrum. Also, because Q/S is not negative at low frequencies, this indicates that shock coalescence is not occurring at 18 m. In Fig. 7, the Q/S calculations for 74 and 150 m suffer from sharp sign changes in the midfrequency region that appear to be related to the earlier discussed spectral dips; however, there is again evidence of nonlinear energy transfer to high and possibly low frequencies.

Conclusions

Analyses of the F/A-18E static engine run-up measurements have indicated that the noise is non-Gaussian and the propagation nonlinear at afterburner and military thrust conditions. Also, calculation of the nonlinearity indicator derived by Howell and Morfe, Q/S , supports the nonlinear propagation hypothesis and calls attention to the indicator itself, which has seen only very limited use since it was derived (see Refs. 2 and 3). Finally, this study has demonstrated that additional and perhaps more extensive investigations in this area are merited. Whereas nonlinear effects do appear to be a factor in the propagation of noise radiated from high-performance jet aircraft, their role has not been defined quantitatively and will likely depend on the propagation environment as well as on source parameters such as jet velocity and temperature.

Acknowledgments

The authors are grateful to Richard McKinley and the U.S. Air Force Research Laboratory for making these measurements possible, as well as to the U.S. Naval Air Engineering Station Lakehurst and the Joint Strike Fighter Program Office for test facility support. A. A. Atchley and T. B. Gabrielson are supported by the U.S. Office of Naval Research. K. L. Gee and V. W. Sparrow are supported by the Strategic Environmental Research and Development Program and Wyle Laboratories.

References

- Blackstock, D. T., "Nonlinear Propagation Distortion of Jet Noise," *Proceedings of the Third Interagency Symposium on University Research in Transportation Noise*, edited by G. Banerian and P. Kickinson, Univ. of Utah, Salt Lake City, UT, 1975, pp. 389–397.
- Morfe, C. L., and Howell, G. P., "Nonlinear Propagation of Aircraft Noise in the Atmosphere," *AIAA Journal*, Vol. 19, No. 8, 1981, pp. 986–992.
- Howell, G. P., "Nonlinear Propagation of Aircraft Noise in the Atmosphere," Ph.D. Dissertation, Faculty of Engineering and Applied Science, Univ. of Southampton, Southampton, England, U.K., May 1982.
- Norum, T. D., Garber, D. P., Golub, R. A., Santa Maria, O. L., and Orme, J. S., "Supersonic Jet Exhaust Noise at High Subsonic Flight Speed," NASA TP-2004-212686, Jan. 2004.
- Gurbatov, S. N., and Rudenko, O. V., "Statistical Phenomena," *Nonlinear Acoustics*, edited by M. F. Hamilton and D. T. Blackstock, Academic Press, San Diego, CA, 1998, Chap. 13.

⁶Ffowcs Williams, J. E., Simson, J., and Virchis, V. J., "Crackle: An Annoying Component of Jet Noise," *Journal of Fluid Mechanics*, Vol. 71, No. 2, 1975, pp. 251–271.

⁷Krothapalli, A., Venkatakrisnan, L., and Lourenco, L., "Crackle: A Dominant Component of Supersonic Jet Mixing Noise," AIAA Paper 2000-2024, June 2000.

⁸Bendat, J. S., *Nonlinear Systems Techniques and Applications*, Wiley, New York, 1998, Chap. 1.

⁹Bass, H. E., Sutherland, L. C., Zuckerwar, A. J., Blackstock, D. T., and Hester, D. M., "Atmospheric Absorption of Sound: Further Developments," *Journal of the Acoustical Society of America*, Vol. 97, No. 1, 1995, pp. 680–683; "Erratum: Atmospheric Absorption of Sound: Further Developments," *Journal of the Acoustical Society of America*, Vol. 99, No. 2, 1996, p. 1259.

¹⁰McInerny, S. A., and Olcmen, S. M., "High-intensity Rocket Noise: Nonlinear Propagation, Atmospheric Absorption, and Characterization," *Journal of the Acoustical Society of America*, Vol. 117, No. 2, 2005, pp. 578–591.

B. Balachandran
Associate Editor

Planar Shock Generator for Wind Tunnels with Circular Cross Section

S. R. Sanderson*

California Institute of Technology,
Pasadena, California 91125

I. Introduction

SHOCK-WAVE interactions are the subject of extensive research in the field of fluid mechanics.^{1–4} A significant difficulty in the conduct of experiments involving shock-wave interactions lies in the generation of the impinging shock wave. At moderately high Mach numbers the oblique shock wave produced by a wedge lies close to the wedge surface, and the distance from the wedge surface to the shock wave at the trailing edge is important in determining the allowable size of the experimental apparatus. Simple wedge shock generators also generate a planar wave over only a fraction of their total width caused by edge effects, and this effect is exacerbated at lower Mach numbers where the edge expansion propagates at a larger angle into the core flow. In the case of wind tunnels with circular cross section, the geometrical layout of a planar wedge shock generator leads to particularly inefficient use of the available space. When viewed in cross section, the leading edge of the wedge cuts a chord across the wind-tunnel cross section. All flow passing below this chord is wasted, along with the fraction of the span contaminated by edge effects, resulting in the use of undesirably small models. Further, because the leading edge of the shock generator is typically positioned well away from the centerline of the test section, the available chord width is significantly less than the full diameter, in addition to allowances made for spillage and edge effects.

II. Description of New Shock Generator

The shovel-shaped shock generator that is illustrated in Fig. 1 represents a response to these difficulties, and the concept is analogous to a class of supersonic lifting body shapes that are known as wave riders.⁵ The shape is generated by inclining a cylindrical tube of arbitrary cross section (circular in the current example; Fig. 1a) at a specific postshock flow deflection angle δ (Fig. 1b). For a given

Received 4 December 2003; revision received 9 January 2005; accepted for publication 11 January 2005. Copyright © 2005 by Simon Sanderson. Published by the American Institute of Aeronautics and Astronautics, Inc., with permission. Copies of this paper may be made for personal or internal use, on condition that the copier pay the \$10.00 per-copy fee to the Copyright Clearance Center, Inc., 222 Rosewood Drive, Danvers, MA 01923; include the code 0001-1452/05 \$10.00 in correspondence with the CCC.

*Graduate Student, Graduate Aeronautical Laboratories; currently New Product Introduction Manager, GE Infrastructure Security, Tualatin, OR 97062.